MUST

Mongolian Geoscientist

THE GEOLOGICAL SOCIETY OF MONGOLIA

Original Article

Climate Change Effects on High Mountain Land Cover: A Case Study of "Ikh Bogd" National Park, Mongolia

Uuganbat Ganbold[1], Ser-Od Tsedevdorj[1]*, Dash Doljin[1], Tsogbadral Khurelbaatar[1], Bat-Erdene Tsedev[1], Amgalan Avkhinsukh[1], Altanbold Enkhbold[2]

[1]*Department of Geography, School of Mathematics and Natural Sciences, Mongolian National University of Education, Ulaanbaatar 14191, Mongolia*
[2]*Laboratory of Geopedology, Department of Geography, School of Arts and Sciences, National University of Mongolia, Ulaanbaatar 14200, Mongolia*

**Corresponding author: serod@msue.edu.mn, ORCID: 0000-0001-5700-908X*

ARTICLE INFO

Article history:

Check for updates

Received 03 May, 2026
Revised 09 July, 2026
Accepted 12 July, 2026

ABSTRACT

This study investigates the impact of climate change on high-mountain land cover dynamics in the Ikh Bogd National Park, Bayankhongor Province, Mongolia, by analyzing summer (June-August) averages for the years 2000, 2005, 2010, 2015, 2020, and 2025. Climatic data indicate a pronounced warming trend, particularly in winter. The absolute maximum temperature in January increased from -6.34°C in 2000 to -0.86°C in 2025, while the absolute minimum temperature rose from -30.4°C to -22.9°C, reflecting a stronger warming in the cold season. Annual precipitation increased substantially from 60.3 mm to 167.1 mm, with recent years showing higher variability and more frequent extreme precipitation events. Vegetation dynamics assessed using Normalized Difference Vegetation Index reveal an overall degradation trend. Maximum Normalized Difference Vegetation Index values declined from approximately 0.39 in 2000 to 0.33 in 2010, alongside decreasing minimum values, indicating reduced vegetation density and increased fragmentation. Although partial recovery was observed in 2015-2025, vegetation remained sparse. Land surface temperature analysis shows elevated surface temperatures, with peak values recorded in 2005 and 2010, and continued warming in high-altitude zones (>3000 m), where temperatures increased by approximately 0.9°C between 2015 and 2025. A moderate negative correlation (r = -0.46) between Land surface temperature and Normalized Difference Vegetation Index suggests that rising temperatures adversely affect vegetation cover, particularly during drought conditions. Between 2000 and 2025, rock cover increased from 18.2% to 41.02%, sparse vegetation decreased slightly from 35.3% to 31.33%, and slight fluctuations were observed for medium and dense vegetation.

Keywords: Climate Change, Land Cover, NDVI, LST, Precipitation

INTRODUCTION

The increasing threat of climate change taxes human aspirations toward a sustainable planet, as the sheer magnitude of the problem and the potential to challenge existing paradigms beyond the thresholds of historical practice make it one of the most complex and far-reaching issues humans have ever encountered (World Bank, 2009; Engle, 2011). The risks and vulnerabilities posed by this climate change in different regions also differ. The term vulnerability is gaining importance as cross-cutting theme in research on the human dimensions of global environmental change (O'Brien et al., 2004; Gbetibouo and Ringler, 2009; Abson et al., 2012; Engle, 2011), especially in environmental policy formulation and development debates (Stelzenmüller et al., 2010). Spatially explicit vulnerability assessment technique is helpful in identifying those groups and susceptible areas to amelioration, allowing more targeted policy and management implementation for mitigating current challenges as well as reducing future risks (Erickson et al., 2014; Abson et al., 2012). Changes in land use and land cover occur as a consequence of the intricate interplay between natural processes and human socio-economic activities (Johnson and Lewis, 2007). These dynamics evolve as a function of the synergistic impacts arising from natural determinants and anthropogenic interventions (Perminova et al., 2016). "We observe a rapid change in land cover over a 25-year period that we consider to be a response to global warming and associated climate change" Land use changes also affect surface temperatures through non-radiative processes, particularly through the hydrological cycle. These processes are less well known and are difficult to quantify but tend to offset the impact of albedo changes. As a consequence, there is low agreement on the sign of the net change in global mean temperature as a result of land use change (Jia et al., 2019; Hartmann et al., 2013; Tsedevdorj et al., 2025).

Climatic and environmental changes negatively influenced the health of the crops in the following ways: variations in rainfall (Kimuku and Ngigi, 2017), extreme heat stress, change in LST, and migration of the peoples from rural to urban areas (Hussain et al., 2020a; Mukherjee and Singh, 2020; Hussain and Karuppannan, 2020b). Land surface temperature (LST) is a critical variable in the Earth's climate system, representing how warm or cold the surfaces on Earth are. LST is an important component of the Earth's energy budget, closely linked to the partitioning between sensible and latent heat fluxes. As such, high-resolution satellite-derived LST is increasingly used in various applications related to the assessment of land surface conditions, including mapping urban extent and the intensity of urban micro-climates, estimating high-resolution evapotranspiration for the management of water resources and assessing vegetation stress (Ermida et al., 2020). Topography affects LST by changing surface illumination conditions under different slopes and aspects. For example, in the Northern hemisphere, the north-facing slopes experience less radiation than the southern ones and therefore have relatively low LST. Vegetation can also affect LST by absorbing and reflecting solar radiation energy and controlling latent and sensible heat exchange. Normalized Difference Vegetation Index (NDVI) is frequently used to investigate the LST relationship with vegetation (Sandholt et al., 2002).

In Mongolia, regional studies were expanded and systematic research began to cover the entire country. Research aimed at distinguishing between natural areas and zones began in the 1950s, with botanist A.A.Yunatov, geographer E.M.Murzaev, and pedologist N.D.Bespalov playing key roles in this field. A.A.Yunatov (1948) distinguished between high mountain areas (taiga), mountain taiga, mountain steppe, steppe, desert steppe, and desert in Mongolia based on vegetation diversity (Batchuluun, 2020). E.M.Murzaev (1952) distinguished the following zones of general geographical regularities: alpine (mountain meadow), mountain taiga, mountain steppe and forest-steppe, high steppe, desert steppe (gobi), and desert. Based on these, Sh.Tsegmid (1969) distinguished the following zones in Mongolia: taiga, taiga zone, forest-steppe, steppe, gobi, and desert zones (Elizabeth, 2012; Batchuluun, 2020). The landscape pattern that occurs in high mountains is vertical zonation. In the mountains of Mongolia, two vertical zonations are distinguished: high mountain and mountain taiga, and in terms of area covered, they are usually included in the forest-steppe zone (Tsegmid, 1969; Dash, 2015; Batchuluun, 2020). The Mongolian Altai Mountains are very different from the forested mountain steppes of Khangai and Khentii. On the one hand, they are extremely susceptible to the effects of cold due to their high absolute altitude, whilst on the other hand, they are also susceptible to the effects of aridity due to their deep penetration into the Gobi and desert regions, and thus directly transition into the Gobi and desert regions, and therefore fall into the steppe zone (Dash, 2015). The Gobi-Altai Mountains (Ikh Bogd), a continuation of the Altai Mountains, are located in the Gobi Desert region and represent a dry and arid region, so the current conditions of soil and plant distribution and landscape patterns are unique (Kappas et al., 2020; Tsedevdorj et al., 2025; Altanbold et al., 2025).

STUDY AREA

The Ikh Bogd mountain was formed ~400 million years ago as a result of the Caledonian orogeny in the northeastern part of Central Asia, where it meets the southwestern extension of the Altai Mountains. Later, ~60 million years ago, the northern passive margin of the Greater Indian plate made contact with the active southern margin of Eurasia. The evolving collision propagated thousands of kilometres north of the plate boundary, eventually reactivating the Gobi-Altai range in the Late Paleogene, and elevating it to one of the peaks of the Altai Mountains (Byamba et al., 2023). The Ikh Bogd is the highest peak in the Gobi-Altai range.

One of the physical geographical features of Mongolia is the distribution of glaciers in the northern and western mountains, including ancient glaciers spread across high mountains such as the Ikh Bogd, which are currently at an altitude of 2,750-4,374 m above sea level (Tsedevdorj, 2021).

The Gobi-Altai range reaches a height of 3,957.0 m at the border of Bogd, Jinst, Bayangovi, and Bayanlig soums in Bayankhongor province (Fig. 1). The mountain range stretches over 50 km in a straight line from the Khuukhen's Khutul eastward to the Uvt-Icheet valley (Baasan, 2008) and over 80 km if the length of Builsan Zadgain Sair is taken into account (Duvjir, 1961). In the Ikh Bogd Mountains, the mountains Tsetsen (2,936.3), Bakhar (2,529.6), Tariat (2,465), and Noyon (2,602) stretch along the border with the Bayantsagaan range, while the mountains Jaran Bogd (2,757), Tsonj (2,364), and Dulaan Bogd (2,565) stretch along the border with Baga Bogd (Davaa et al., 2008; Tsedevdorj et al., 2024).

Starting from the late 19th century, Russian and American researchers M.V.Pevtsov (1878-1879), G.N.Potanin (1884-1886), D.A.Klementz (1883-1896), V.A.Obruchev (1899), P.K.Kozlov (1923-1925), and R.C.Andrews (1923-1926) conducted research and descriptions of ancient geography, landscape, geomorphology, geology, stratigraphy, tectonics, geological history, glacial sediments, and paleontology in the region (Tsegmig, 1969; Bayasgalan et al., 1999; Tsedevdorj et al., 2024). Some spring waters of the Ikh Bogd National Park and Lake Orog were analysed, and it was

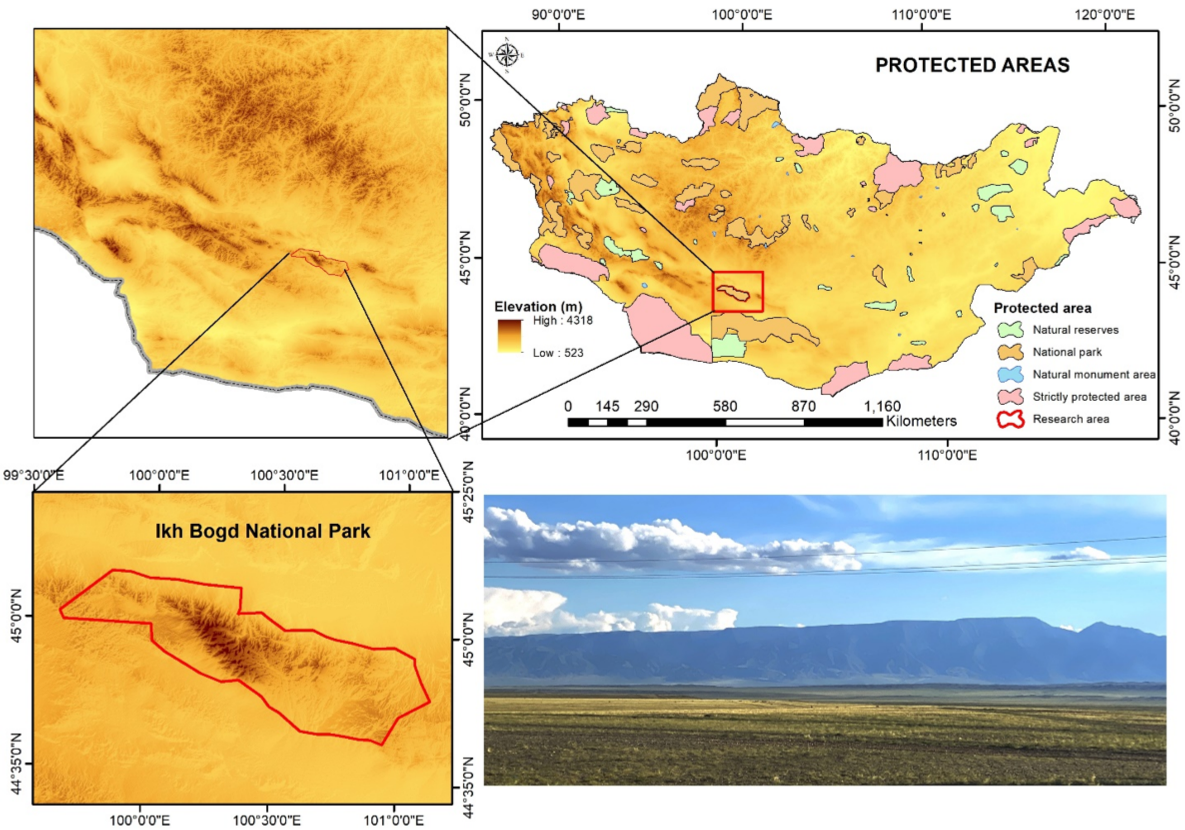

Fig. 1. Study area map of district Ikh Bogd National Park

determined that the lakes of the lake valley were once significantly larger than their present-day size (Smirnov, 1932). It was also found that the geomorphology around the mouth of the Bituut river in the Ikh Bogd Mountains has the characteristics that point to past glaciation, with glacially-scoured gorges and abundant glacial moraine deposits (Simukov, 1936; Rachkovsky and Lebedov, 1932), while Murzaev and Tsegmid visited the region around Lake Orog and studied the ancient geography, changes in the lakes, and the historical climate of the depression between the Gobi-Altai and Khangai mountain ranges (Murzaev, 1952; Badarch et al., 1965).

Both the strike-slip system along the northern edge of Ikh Bogd and the thrust system south of it ruptured in 1957 in a large earthquake, assigned magnitudes from 7.9 to 8.3 (Florensov and Solonenko, 1963). Gobi-Altai earthquake of 1957 December 4 (published magnitudes range from 7.8 to 8.3). The Bogd fault is 260 km long and can be subdivided into five main geometric segments, based on variation in strike direction (Rizza et al., 2011). The 1957, M_W 8.1, Gobi-Altai earthquake, Southern Mongolia, produced a ~360-km-long surface rupture along the Eastern Bogd fault. Cumulative offsets of geomorphic features suggest that the Eastern Bogd fault might produce characteristic slip over the last seismic cycles (Kurtz et al., 2018).

A detailed analysis of the rupture patterns and slip changes along the surface rupture associated with the 1957 Gobi-Altai earthquake (M_W= 8.1) in Mongolia, which occurred along the Bogd left-lateral strike-slip fault, was carried out to better understand segmentation and propagation (Choi et al., 2012). Oyu, Nomin, and Binderya, which were formed by the 1957 magnitude 8.1 earthquake in the Gobi-Altai Range in southern Mongolia. The earthquake blocked a narrow valley, triggered rockfalls, and triggered large rockfalls that disrupted hydrological connectivity in this arid mountainous region (Enkhbold et al., 2026).

This fault is clearly visible in today's landscape. To explain the aforementioned earthquake, V.A.Bobrov and other researchers conducted geographical and geological studies and wrote scientific articles and books, including "Earthquakes in the Gobi Altai" (Bobrov et al., 1959), "Ikh and Baga Bogd" Physical Geographical Description (Duvjir, 1961), "Gobi-Altai Earthquake" (Florensov and Solonenko, 1963), and the seminal geological paper "Forebergs, floral structures, and the development of large intracontinental faults: the Gurvan Bogd fault system in Mongolia" (Bayasgalan et al., 1999).

While early research on the Ikh Bogd National Park was comprehensive and covered all areas, Russian scientists began conducting specialized studies on soils and vegetation in the early 20th

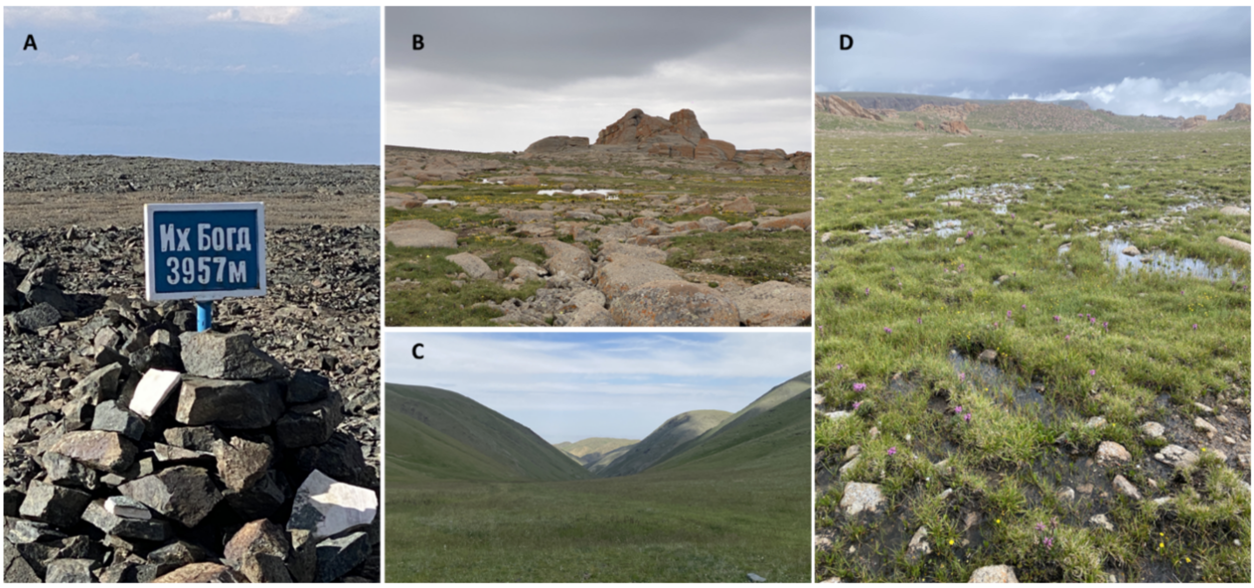

Fig. 2. Surface characteristics of the study area. A) Undeveloped surface of the summit of Ikh Bogd National Park, B) Highly weathered and eroded high mountain cape, C) High mountain steppe, D) High mountain meadow with swamps

Century and gathered a wealth of results (e.g., Kozlov, 1925; Simukov, 1936). In the second half of the 20th century, studies on vertical vegetation zoning were conducted by A.A.Yunatov (1948), N.Ulziikhutag (1989), and W.Hilbig (1995), with soil studies by N.D.Bespalov (1951), D.Dorjgotov, (2003), and studies on crops by Terbish and Jamsran (2006). In 2025, Tsedevdorj et al. conducted field research in the study area to identify landscape change.

Within the framework of this study, investigations were carried out to determine variations in soil characteristics and vegetation composition of the mountain system, while also integrating geological and geomorphological analyses. In addition, geomorphological features such as faulting and landslides formed as a result of the 1957 earthquake were documented, and their influence on the present-day landscape was assessed. Furthermore, the impact of climate change on these processes and on land cover dynamics was also examined (Fig. 2).

MATERIALS AND METHODS

Remote sensing data

Archive Landsat images of 30 m × 30 m spatial resolution covering the study area were collected from the years 2000, 2005, 2010, 2015, 2020 and 2025. The imagery was downloaded from the United States Geological Survey website (https://earthexplorer.usgs.gov/) with mixed vegetation, an agricultural area, and bare surface as mapped Land Use and Land Cover (LULC) types (Rani et al., 2018). Thermal Infrared Sensing (TIRS) images were acquired from June to August 2000, 2005, 2010, 2015, 2020 and 2025, and were relatively free of clouds and haze. The Landsat images were processed using ArcGIS 10.8 and Google Earth Engine.

Estimation of NDVI

The NDVI was used to assess changes in vegetation cover. NDVI is based on the difference between near-infrared (NIR) and red (Red) reflectance and is calculated as per. In this study, surface reflectance data from Landsat 7 ETM+ and Landsat 8 OLI Collection 1, 2 Level-1, 2 products were used (Fig. 3).

Estimation of Land cover

Land cover (LC) was classified using Google Earth Engine using random forest based on Landsat 7 and 8 images. Composites of Landsat 8 images filtered by date and cloud cover (<10%) were median filtered for atmospheric correction and then cropped to regions of interest (ROI). Cloud masks were used during preprocessing to ensure data quality (Fig. 4).

Estimation of LST

The LST is a general term describing the joint temperature of complete objects existing on the Earth's surface. Different researchers have used defined measurements on Landsat data to compute the LST. The LST values were estimated from the TM, TM+, and OLI thermal bands (band

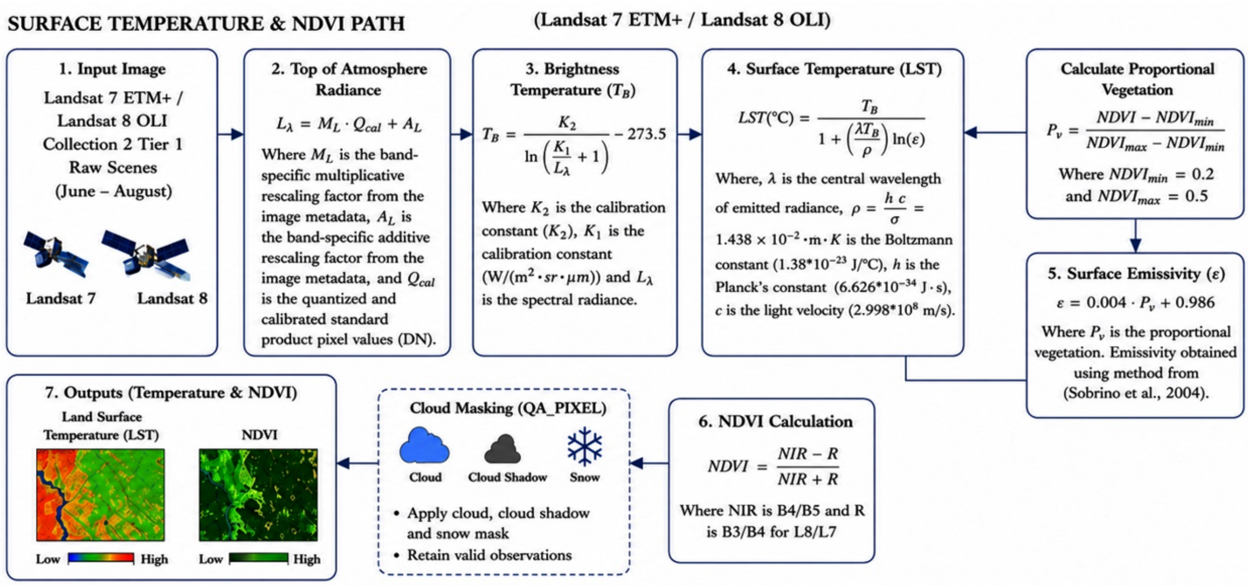

Fig. 3. The flowchart represents the step-by-step procedure for estimating NDVI and LST

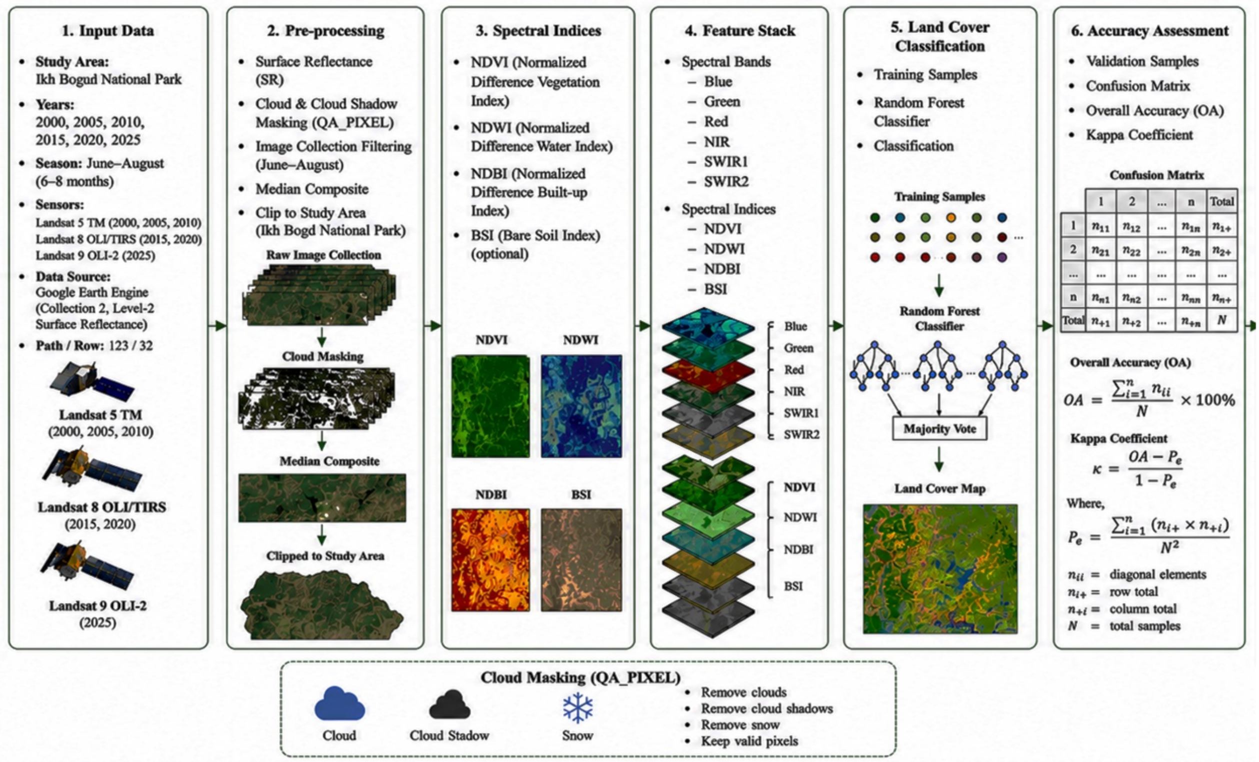

Fig. 4. The flowchart represents the step-by-step procedure for estimating land cover

6 and band 10). All steps for calculation of LST are given below (Bento et al., 2018) in Fig. 3.

Climate change data

Climate variables, including temperature and precipitation, were obtained from the NASA POWER database. Finally, statistical analyses were conducted to examine the relationships between climate variability and land cover change over the 25-year study period.

RESULTS

Minimum temperatures have increased (winters have warmed) during the study period. Precipitation is generally increasing, with the highest values in 2015 and 2025. Maximum summer temperatures vary between years, with the highest valuesin 2010 and the lowest values in 2015. Therefore, warming and precipitation increases are observed simultaneously in the region (Table 1).

In 2000, the absolute minimum air temperature ranged from -30.4 to -9.02°C (January-April), -3.4 to -0.26°C (May-September), and -13.0 to -12.0°C (October-December), whereas in 2025, it ranged from -22.9 to -7.52°C, -1.2 to +0.42°C,

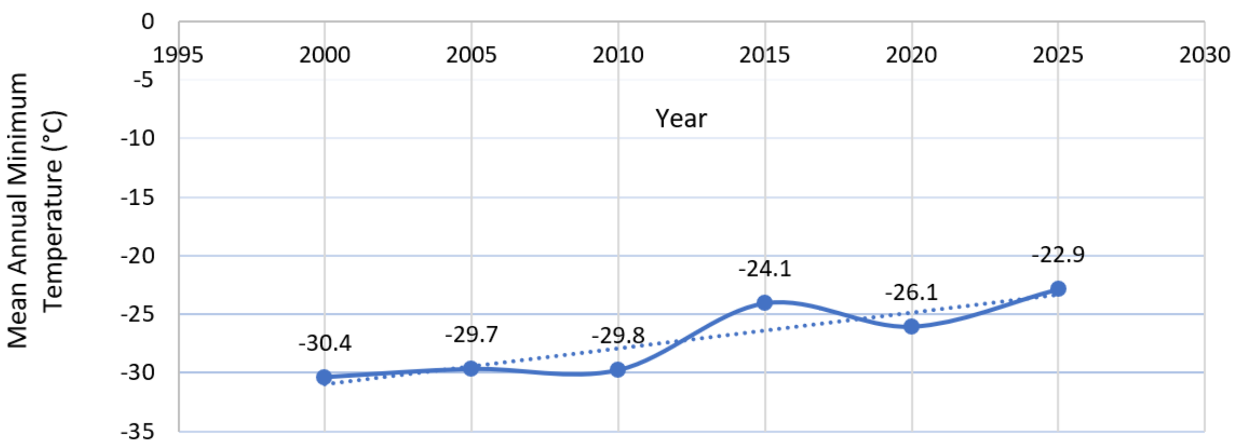

Fig. 5. The trend of the annual minimum temperature from 2000 until 2025 for Ikh Bogd National Park, Mongolia

Table 1. Historical monthly weather data

Year/ month	1	2	3	4	5	6	7	8	9	10	11	12
2000 max	-6.34	1.53	17	21	28.5	30.6	36.1	28.82	28.2	17.9	4.15	16.8
2000 min	-30.4	-24	-19	-9.02	-3.4	5.57	8.94	3.68	-0.26	-13	-22.9	-12
2000 prec	1.83	1.5	1.94	2.4	3.81	5.46	17.8	15.62	1.15	6.24	1.43	2.94
2005 max	-5.14	-1.4	14.1	25.9	24.7	34.2	36.2	30.69	29	17.9	8.57	18.5
2005 min	-29.7	-29	-21	-7.12	-5.8	2.16	9.42	4.13	-2.21	-6.7	-15.9	-8.3
2005 prec	2.21	2.96	0.33	1.73	10.2	10.05	20.1	32.47	10.8	3.33	1.75	5.29
2010 max	1.56	5.64	17.4	22.2	24.7	35.1	36.5	30.56	28	21.5	9.16	19.5
2010 min	-29.8	-28	-26	-14.7	-4.3	0.59	9.75	3.71	-2.06	-6.7	-18.6	-9.1
2010 prec	1.83	1.36	1.69	8.2	19.6	21.59	20.9	8.1	15.8	2.36	1.07	6.4
2015 max	-0.33	5.58	15.1	26.5	26.8	29.7	31.8	31.31	24.5	19.2	9.57	17.7
2015 min	-23.1	-24	-20	-9.02	-3.8	1.06	7.75	4.4	-4.58	-9	-19.3	-11
2015 prec	1.14	2.05	0.81	9.53	9.47	58.48	23.1	11.8	33.1	4.04	5.48	14.2
2020 max	0.03	8.87	13.5	28.6	28.6	32.1	31.8	30.63	27.5	13	7.34	15.9
2020 min	-20.5	-21	-17	-6.79	-1.7	2.65	9.63	5.55	-1.51	-6.7	-18.5	-8.9
2020 prec	1.18	1.17	1	1.14	16.4	8.78	27.1	13.06	22.5	0.25	5.64	9.47
2025 max	0.86	6.05	15.3	21.2	29.9	30.4	33	30.93	25.9	21.3	10.2	19.1
2025 min	-22.9	-22	-15	-7.52	-1.2	2.59	9.8	5.65	0.42	-14	-20.2	-11.2
2025 prec	0.34	0.15	5.87	4.49	27.6	32.6	39.3	19.22	21	4.67	9.46	11.7

and -14.0 to -11.2°C for the respective periods (Table 1). A warming trend in absolute minimum air temperature is evident for the period 2000-2025, with the strongest signal observed in winter. The minimum temperature in January decreased from -30.4°C in 2000 to -22.9°C (+7.5°C) in 2025, indicating that extreme cold conditions are weakening and the minimum temperature regime is trending upward. During the winter months of 2000, 2005, and 2010, absolute minimum temperatures ranged between -30.4°C and -28.0°C, whereas in the period 2015-2025 they stabilized between -23.1°C and -22.0°C. This indicates a consistent upward shift in the lower threshold of extreme cold conditions over time. A similar trend is also observed during the warm season. Specifically, the minimum temperatures in July and August increased by +0.86°C to +1.98°C in 2025 compared to 2000, suggesting a reduction in nocturnal cooling and an overall rise in minimum temperature levels during the warm season. This pattern indicates that not only are seasonal mean temperatures increasing, but the lower bound of the diurnal temperature range is also shifting toward warmer conditions (Fig. 5).

The mean July maximum temperature for 2000-2025 was +34.2°C. Maximum temperatures ranged from +27.1 to +27.2°C during May-September, +18.4 to +24.2°C in April-October, and +4.34 to +17.9°C in December-February (Table 1). Winter (December-February) maximum temperatures ranged from +4.34 to +17.9°C. Table 1 further indicates an increasing trend in maximum air temperatures over 2000-2025, consistent with the observed rise in minimum temperatures and suggesting year-round warming in the study area. The mean absolute maximum air temperature in July reached +34.2°C during the study period, confirming that peak annual temperatures consistently occur in mid-summer. Temperatures during May-September remained stable, ranging narrowly between +27.1°C and +27.2°C, while transitional months (April and October) exhibited broader variability between +18.4°C and +24.2°C. Overall, these patterns indicate a relatively stable seasonal thermal regime, with a discernible shift toward warming conditions. A clear increase in absolute maximum temperatures is also observed during the winter season. For instance, the absolute

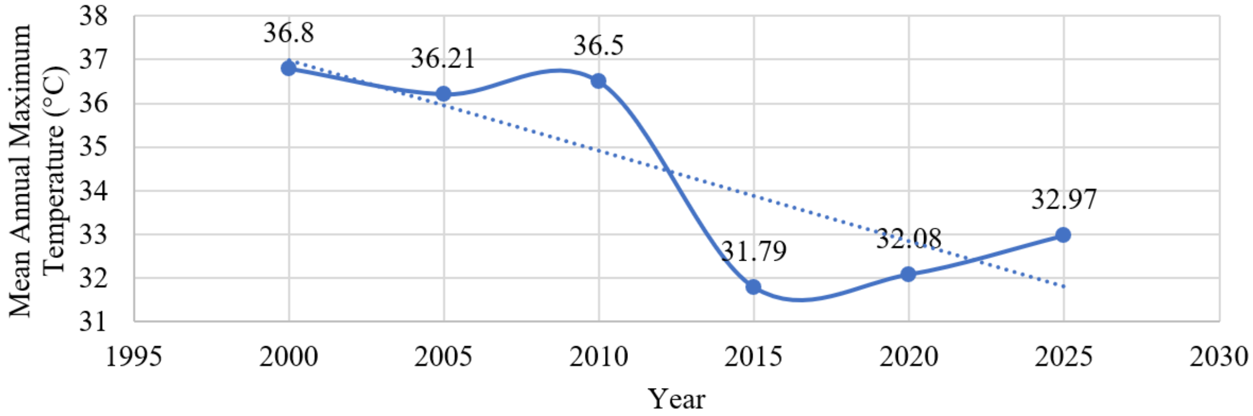

Fig. 6. The trend of the mean annual maximum temperature from 2000 until 2025 for Ikh Bogd National Park, Mongolia

maximum temperature in January increased from -6.34°C in 2000 to -0.86°C in 2025, representing a rise of 5.48°C. Similarly, January and February temperatures in 2025 were higher by approximately 4.52-5.48°C compared to 2000. These results indicate a weakening of winter cold intensity and suggest a more pronounced warming trend during the cold season (Fig. 6). These changes indicate that not only minimum temperatures but also maximum temperature values were increasing across the 25-year period of this study, suggesting an upward shift in the entire range of extreme temperatures in the study region. In other words, the warmest winter days have become significantly warmer than in the past, while the warmest summer days have remained consistently higher, as shown in Figs. 5, 6 and Table 1. Therefore, the increase in absolute maximum temperatures observed between 2000 and 2025 is a key indicator of climate change, with warming particularly evident in winter. This trend has important implications for snow and ice formation, the seasonal dynamics of soil freezing, the growth period of vegetation, and the seasonal regime of water resources.

Overall, the observed increase in absolute maximum temperatures, together with the changes in absolute minimum temperature values over the 25-year period, clearly indicates a period of climate warming in the study area. Notably, the greater rise in minimum temperatures during winter suggests that warming in the cold season is more pronounced than in the warm season. These findings provide robust evidence of ongoing climate change in the region and imply potential impacts on snow cover, soil freezing processes, hydrological regimes, and the seasonal dynamics of ecosystems.

The total annual precipitation increased from 60.3 mm in 2000 to 167.1 mm in 2025, an increase of 106.8 mm over a 25-year period. This is equivalent to an increase of approximately 2.8 times, indicating a significant change in the regional moisture regime. In terms of temporal variability, the annual precipitation gradually increased from 60.3 mm in 2000 to 104.9 mm in 2010. A significant increase was observed in 2015, reaching 160.5 mm, and then temporarily decreased to 98.79 mm in 2020. However, by 2025, the precipitation had increased again to 167.1 mm. Such variability indicates a high level of interannual variability, indicating that the precipitation regime in the region is unstable. Analysis of the monthly distribution shows that the majority of precipitation is concentrated between June and September. In 2025, the peak precipitation was recorded in July and August, with total monthly precipitation reaching 39.3 mm in July, 32.6 mm in June, and 27.6 mm in May (Fig. 7). This pattern is consistent with the continental climate of Mongolia, where the majority of annual precipitation occurs during the summer season. Furthermore, the results suggest an increasing likelihood of short-duration, high-intensity precipitation events during summer. Precipitation remains minimal during the dry winter months (November-February) and early spring, typically ranging between 0.15 and 2.5 mm. Notably, only 0.15 mm of precipitation was recorded in February 2025, indicating extremely dry conditions. Although relatively high precipitation (21.59 mm) was observed in

Fig. 7. The trend of the mean annual precipitation from 2000 until 2025 for Ikh Bogd National Park, Mongolia

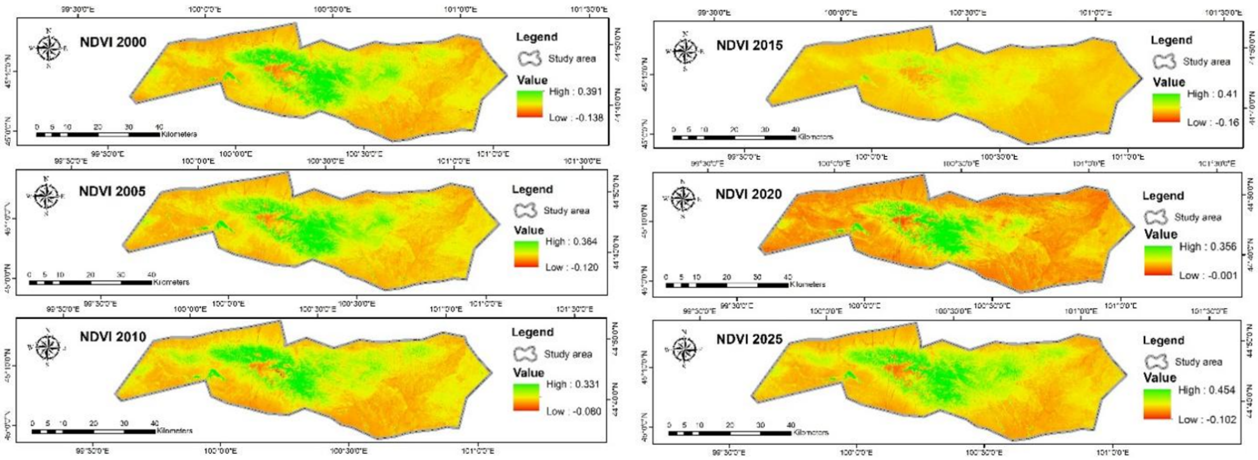

Fig. 8. NDVI maps of Ikh Bogd National Park for 2000, 2005, 2010, 2015, 2020 and 2025

June 2010, the overall low precipitation during the remaining months suggests a potential linkage with higher LST and NDVI in that year. In contrast, the consistently higher precipitation recorded between May and September 2025 (21.0-39.3 mm) appears to be a key factor contributing to the elevated NDVI values observed during the same period, indicating enhanced vegetation growth.

Monthly precipitation analysis shows that 45.3 mm was recorded in July 2000, whereas the highest monthly precipitation occurred in August 2021, reaching 57.2 mm. In 2010, relatively higher snowfall was observed during the January-May period, while precipitation levels remained nearly uniform during the summer months (June-August). At five-year intervals, precipitation patterns exhibit considerable variability; however, a comparison between 2000 and 2021 indicates an overall increase of approximately 18.9 mm (around 11%), suggesting a general upward trend influenced by interannual climatic conditions. Overall, precipitation in the Ikh Bogd National Park protected area shows substantial year-to-year variability over the period 2000-2025. The increased summer precipitation observed in 2025 appears to have positively influenced vegetation recovery, whereas the pronounced fluctuations observed in 2010 and 2015 likely exerted stress on the regional ecosystem.

A pronounced seasonal pattern is evident, with precipitation predominantly concentrated during the summer months (June-August). In particular, July consistently exhibits the highest values across all years. In contrast, precipitation during winter (November-February) and early spring remains minimal and relatively stable. Interannual variability is marked by the occurrence of pronounced peaks in certain years, notably in 2015 and 2025, when extreme monthly values were recorded (e.g., 58.48 mm and 39.30 mm in June-July). Compared to the early period (2000-2005), summer precipitation during recent years (2015-2025) shows an overall increasing trend. The uneven distribution of precipitation suggests that, in some years (e.g., 2010 and 2015), rainfall is highly concentrated within specific months, indicating the dominance of short-duration, high-intensity rainfall events. Furthermore, the increasing frequency of higher precipitation extremes in recent years may reflect the influence of climate change, suggesting enhanced variability in precipitation patterns. In other words, although total precipitation does not exhibit a strictly stable trend, there is a clear tendency toward the dominance of extreme events (Fig. 7).

The maximum NDVI value declined gradually from approximately 0.39 in 2000 to ~0.36 in 2005 and ~0.33 in 2010. Similarly, minimum values also decreased (from ~0.14 to ~0.12 and ~0.08), indicating an overall reduction in vegetation cover. In subsequent years, NDVI values exhibited fluctuations, with maximum and minimum recorded as 0.417 and -0.165 in 2015, 0.356 and -0.001 in 2020, and 0.454 and -0.102 in 2025, respectively (Table 2).

Despite these variations, a general trend of vegetation degradation is evident. In 2005, relatively dense vegetation (high NDVI values) was more spatially extensive; however, by 2010, these areas had contracted and become increasingly fragmented. This pattern suggests a decline in vegetation density and a potential degradation of the ecosystem. Spatially, higher NDVI values in 2000 were concentrated in the central and northern parts of the mountainous system, likely associated with greater moisture accumulation on mountain foothills and leeward slopes. In contrast, lower NDVI values were observed on the southern slopes and western areas, where sparse vegetation, dry conditions, and rocky surfaces dominate. Notably, the minimum NDVI value of -0.138 indicates the presence of extremely dry, water-deficient areas with little to no vegetation cover. Compared to 2000, the maximum NDVI value in 2010 decreased by 0.06 units, reflecting a decline in photosynthetic activity and green biomass within the densest vegetation zones over the decade. Conversely, the minimum NDVI value increased to -0.080, suggesting a reduction in the intensity of negative values and indicating possible partial recovery in sparsely vegetated areas. A comparison between 2015 and 2020 shows a further decrease in the maximum NDVI value by 0.061 units, implying a slight reduction in vegetation density. However, the spatial extent of vegetation appears to have expanded, particularly in the central-southern mountainous regions. Importantly, the minimum NDVI value reached -0.001 in 2020, approaching zero, which represents a significant shift compared to previous years. This suggests a reduction in extremely barren areas and the emergence of sparse vegetation across previously unvegetated surfaces (Fig. 8).

LST dynamics in the study area were analyzed using the average values for the summer months (June-August) for each year.

The highest LST values, reaching 54.2°C, were recorded in 2005 and 2010. In the central mountainous region above 3,000 m, which

Table 2. Dynamic change of NDVI, 2000-2025

Year	NDVI (High value)	Status
2000	0.391	Baseline
2005	0.364	Decline
2010	0.331	Decline
2015	0.417	Growth
2020	0.356	Decline
2025	0.454	Recovery

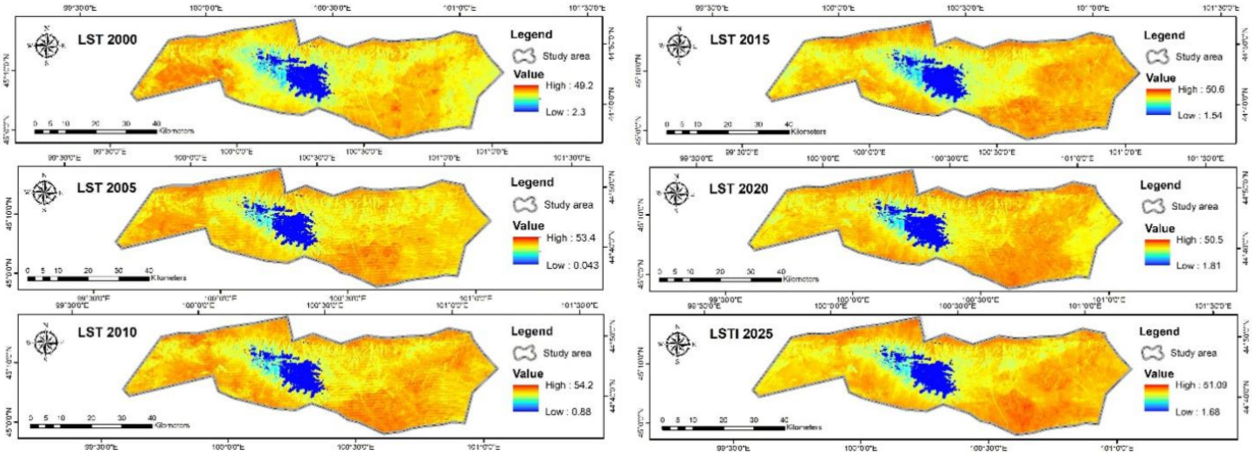

Fig. 9. LST maps of Ikh Bogd National Park for 2000, 2005, 2010, 2015, 2020 and 2025

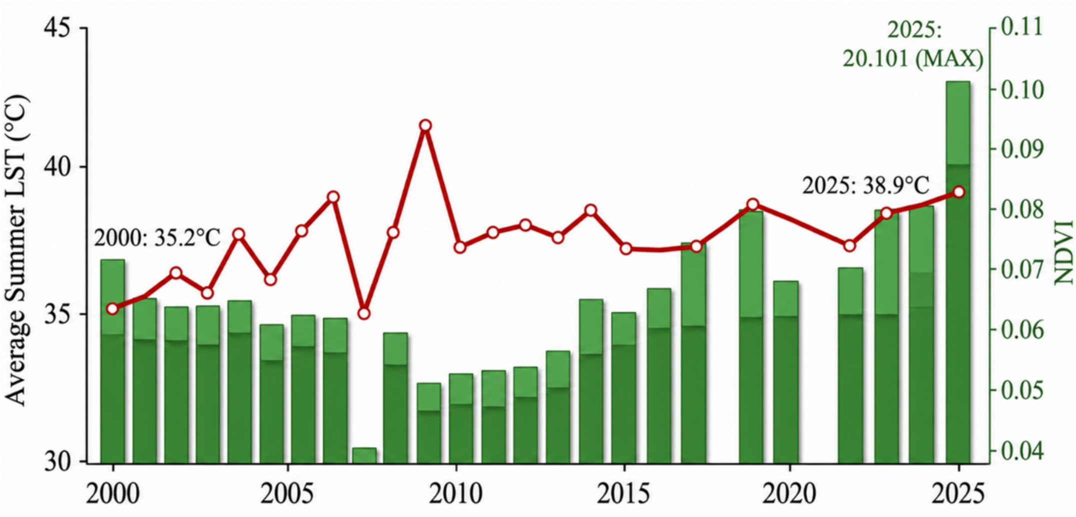

Fig. 10. Relation between NDVI and average summer LST (C)

encompasses the highest peaks of the Ikh Bogd National Park, LST rose from 0.88°C to 1.81°C between 2015 and 2025, indicating a warming of approximately 0.9°C. Consistent with the altitudinal lapse rate (~0.6°C per 100 m), these high-elevation areas exhibit the lowest temperatures, ranging from 2.3°C to 0.043°C. By contrast, the mountain foothills, lowlands, and surrounding desert-steppe regions show significantly higher temperatures, largely due to sparse vegetation cover and increased soil heat absorption. The minimum LST increased from 1.54°C in 2015 to 1.81°C in 2020, suggesting intensified melting of permafrost and seasonal snow cover in high-altitude zones. Overall, the 25-year dynamics (2000-2025) indicate a general warming trend in LST across the Ikh Bogd National Park, posing a significant challenge to the fragile high-mountain desert ecosystem (Fig. 9).

A moderate negative correlation (r = -0.46) was observed between LST and NDVI during the study period. Notably, in 2010, when LST reached its highest value (41.4°C), NDVI declined to its lowest level, indicating a negative impact of elevated temperatures on vegetation cover. This relationship suggests that heat stress and aridity exert a strong influence on the regional ecosystem. However, in 2025, despite relatively high temperatures, NDVI values increased, implying the influence of additional factors, most likely increased precipitation, has affected vegetation dynamics (Fig. 10).

Field surveys conducted in 2025, as part of this study, documented the diversity of land cover types within the study area. The corresponding image clearly distinguishes between sparsely vegetated zones, bare surfaces with no vegetation, areas of moderate to dense vegetation, and rocky terrain. This field-based documentation provides essential ground-truth data for validating the

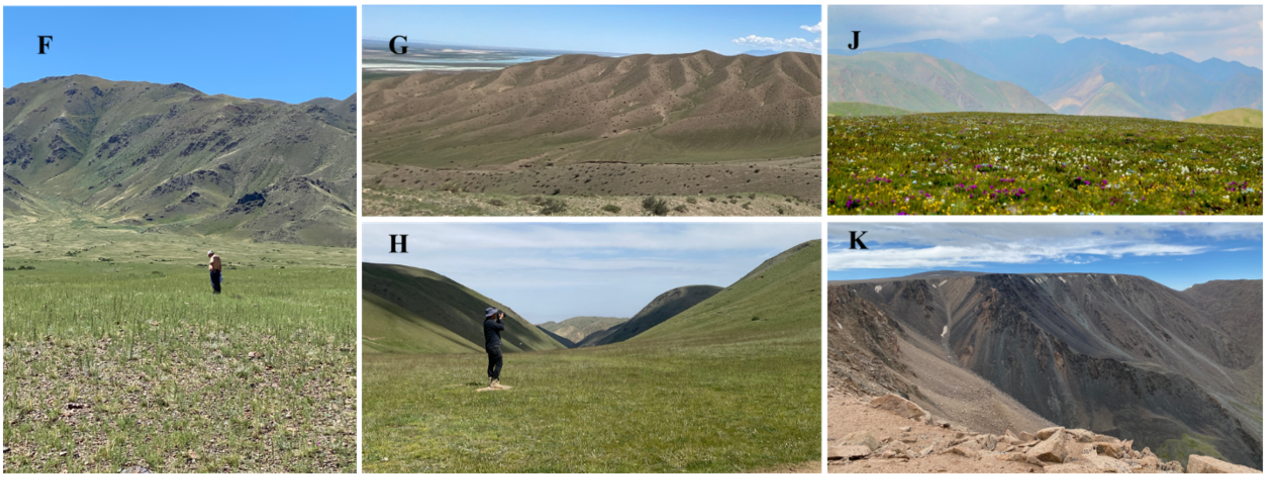

Fig. 11. Land cover classes: F) Sparse vegetation, G) Bare soil, H) Medium vegetation, J) Dense vegetation, K) Rock (Photo by Tsedevdorj, 2025)

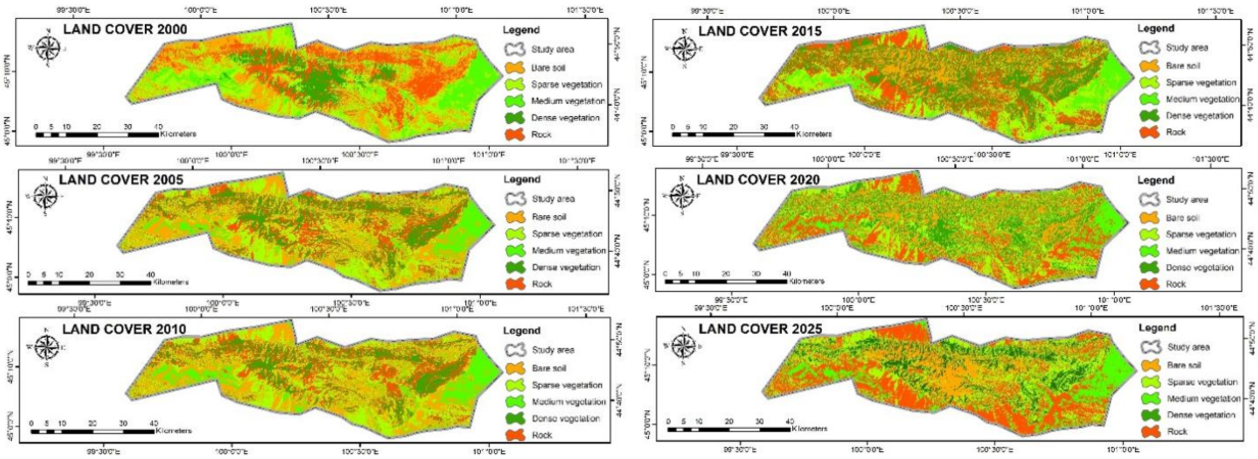

Fig. 12. LC maps of Ikh Bogd National Park for 2000, 2005, 2010, 2015, 2020 and 2025

classification and interpretation of remote sensing datasets. Furthermore, it offers direct evidence of the spatial heterogeneity and distribution of land cover types across the study region (Fig. 11).

There has been a significant change in land cover across the study area. Bare soil has the largest change in the total area. This indicates that vegetation cover has recovered or rocky surfaces have become more dominant. Sparse vegetation remained the dominant land cover class throughout the study period, accounting for 35.3% of the total area in 2000 and 31.33% in 2025. Although its proportion decreased slightly, it continued to represent the largest share of the landscape, indicating relatively stable spatial distribution. Medium vegetation showed a fluctuating trend. Its coverage decreased from 24,005.3 ha (9.1%) in 2000 to 13,176.0 ha (5.0%) in 2015, followed by a gradual recovery to 30,302.9 ha (11.53%) in 2025. This pattern suggests partial vegetation regeneration during the later years of the study period. Dense vegetation exhibited the greatest temporal variability. It increased markedly from 12,681.3 ha (4.8%) in 2000 to 72,911.7 ha (27.7%) in 2015, before declining to 30,680.7 ha (11.67%) by 2025. These fluctuations may reflect interannual climatic variability, ecological succession, or changes in land use and management practices. In contrast, the rock class showed a continuous increase, rising from 47,928.2 ha (18.2%) in 2000 to 107,813.2 ha (41.02%) in 2025, making it the second dominant land cover type by the end of the study period. This increase may indicate enhanced exposure of bedrock due to soil erosion, land degradation, or a reduction in vegetation cover (Fig. 12; Table 3).

DISCUSSION

This study compared changes in average absolute maximum and absolute minimum air temperatures and precipitation data with a 5-year frequency between 2000 and 2025 within the Ikh Bogd

Table 3. LC areal distribution from 2000 until 2025 in Ikh Bogd National Park, Mongolia

Classes	2000		2005		2010		2015		2020		2025	
	ha	%	ha	%	ha	%	ha	%	ha	%	ha	%
Bare soil	85352.1	32.5	60499.1	23.0	65063.9	24.8	22221.9	8.5	18385.6	7.0	11710.8	4.46
Sparse vegetation	92888.1	35.3	92032.0	35.0	89086.7	33.9	69235.8	26.3	89405.9	34.0	82347.4	31.33
Medium vegetation	24005.3	9.1	15640.1	6.0	23311.7	8.9	13176.0	5.0	17220.6	6.6	30302.9	11.53
Dense vegetation	12681.3	4.8	31098.1	11.8	25385.3	9.7	72911.7	27.7	57537.7	21.9	30680.7	11.67
Rock	47928.2	18.2	63585.7	24.2	60007.4	22.8	85309.5	32.5	80305.1	30.6	107813.2	41.02
Total	262855	100.0	262855	100	262855	100	262855	100	262855	100	262855	100

National Park. Also, the normalized vegetation index, LST, and land cover classification were developed based on Landsat satellite data. There are many studies on climate change, normalized vegetation index, and land cover in the entire territory of Mongolia. However, there is a lack of work done on the scale of small specially protected areas.

Our results underscore the strong seasonal and spatial variability in vegetation responses to climate variability and extremes in Mongolia. While the observed climate change trends indicate a prolonged vegetation season and increased precipitation in summer months, changes in NDVI and GPP cannot be explained solely by climate variables. Vegetation dynamics are shaped by both climatic and non-climatic factors, such as grazing and land degradation (Kilpys et al., 2025).

Changes in the NDVI are often used as indicators of the degree of desertification development. However, many studies on this aspect only focus on the trend of vegetation change and rarely pay attention to the state of the region before the change (Filei et al., 2018; Lee et al., 2019). The following conclusions are drawn from the analysis. First, the differences in the NDVI changes obtained using MODIS data between 2000 and 2010 lead to differences in the correlation between NDVI and climate variables. During the study period, NDVI was strongly correlated with precipitation and moderately correlated with temperature. The temporal changes in the mean spatial pattern of NDVI at most stations were most strongly influenced by changes in the average precipitation during the growing season in Mongolia (Narangarav and Lin, 2011). The decline in NDVI to its lowest level (0.356) in 2020 supports the notion that reduced precipitation leads to a contraction of pasture areas. In contrast, the increase in NDVI to 0.454 in 2025 aligns with the observed rise in temperature and precipitation, reflecting a broader trend of vegetation recovery and expansion of sparsely vegetated areas.

Partial least squares (PLS) and random forest (RF) regression models were applied to estimate monthly average near-surface air temperature (Ta) in Mongolia for the period 2002-2017 using Moderate Resolution Imaging Spectroradiometer (MODIS) LST time-series products and terrain parameters. Using only day/nighttime LST and elevation as predictor variables, the correlation between measured and estimated monthly average Ta root-mean-square error (RMSE) ranged from 1.20°C to 2.19°C for the partial least squares regression (PLSR) and 0.84°C to 1.93°C for the RF. Using only day/nighttime LST and elevation as predictor variables, the correlation between measured and estimated monthly average Ta (RMSE) ranged from 1.20°C to 2.19°C for the PLSR and 0.84°C to 1.93°C for the RF (Otgonbayar et al., 2019). Previous studies have examined land cover change in Mongolia using multi-class classification approaches, such as the nine-category scheme applied for the 2001-2015 period (Amarjargal et al., 2017). During the past several decades, desertification and land degradation have become more and more serious in Mongolia. Obtained year-by-year land use/cover changes in Mongolia from 1990 to 2021 using Landsat TM/OLI data. The results show that 17.6% of the land surface has changed at least once among the six land categories from 1990 to 2021. While the area of barren land has significantly increased, the grassland and forest areas have exhibited a decreasing trend in the past 32 years (Hao et al., 2023)

The region selected in this study is characterized by a unique climatic setting, making it particularly sensitive to natural drivers of land cover change. In years with low precipitation, pasture areas tend to decline significantly, accompanied by an expansion of bare surfaces. However, recent trends suggest a reversal of this pattern, with increasing air temperature and precipitation contributing to a reduction in bare land and an expansion of sparsely vegetated areas.

These findings indicate that land cover in the study area responds dynamically to changes in temperature and precipitation regimes. This suggests that the Ikh Bogd National Park is highly sensitive to climatic variability, yet possesses a relatively strong capacity for recovery under improved moisture conditions.

This research should focus on the use of operational satellites to create a certain level of ecological change, the value of which lies in the sustainable management of the area. Advances in remote sensing techniques, particularly in spatial resolution, offer new opportunities to better characterize the structural and functional aspects of ecosystems across multiple scales (Caballero et al., 2022; Cabello et al., 2018). The findings of this study provide a foundational basis for further research and highlight the importance of integrating high-resolution remote sensing data in future ecological assessments of the region.

CONCLUSIONS

-Between 2000 and 2025, the Ikh Bogd National Park Protected Area experienced significant climatic warming, with winter maximum temperatures increasing by 5.48°C and minimum temperatures by 7.5°C, indicating an intensification of regional climate change.

-Annual total precipitation increased from 60.3 mm to 167.1 mm over the 25 years, while recent years (2015-2025) showed more frequent and intense extreme precipitation events, reflecting changes in the regional precipitation regime.

-Long-term NDVI analysis revealed an overall decline in vegetation cover density, as previously continuous high-productivity vegetation zones became reduced and fragmented, suggesting ecosystem degradation.

-LST generally decreased with altitude; however, even areas above 3000 m showed measurable warming, demonstrating that climate change is affecting high-mountain ecosystems as well.

-A moderate negative correlation (r= -0.46) was observed between LST and NDVI, indicating that rising surface temperatures and associated drought conditions have a negative impact on vegetation cover in the study region.

-Overall, the results indicate significant land cover changes from 2000 to 2025, with decreasing bare soil, increasing rock exposure, and fluctuating vegetation cover, suggesting the influence of both climatic and environmental factors.

ACKNOWLEDGEMENTS

We would like to express our sincere gratitude to all the organizations and individuals who supported the implementation of this study. We would also like to express our special gratitude to the project consultant, the teachers and researchers of the Department of Geography of the Mongolian National University of Education. We would like to express our gratitude to the administration of the Ikh Bogd Specially Protected Area and the conservationists for their valuable contribution to the research work. Furthermore, we gratefully acknowledge the financial support provided by the Science and Technology Fund of Mongolia for the implementation of this study.

This study was carried out under the basic research projects “Remote sensing study of landscape transformation and changes in the Ikh Bogd Natural Park” supported by the Mongolian Foundation for Science and Technology and implemented during 2024-2026 (grant no. STF-2024/08) and “Assessment of climate change-induced disaster events and adaptive capacity in high-mountain regions: Case study of Tsambagarav mountain” supported by the Mongolian National University of Education, Mongolia (No.MNUE2026A002)

Authorship

Uuganbat Ganbold: Conceptualisation, Data curation, Formal analysis, Investigation, Methodology, Software, Visualisation, Field data collection, Validation, Writing - Original draft, Writing - Review and editing, Ser-Od Tsedevdorj: Investigation, Field data collection, Data curation, Formal analysis, Methodology, Funding acquisition, Writing - Review and editing, Dash Doljin: Investigation, Field data collection, Data curation, Formal analysis, Tsogbadral Khurelbaatar: Field data collection, Writing - Review and editing, Bat-Erdene Tsedev: satellite data analysis, Amgalan Avkhinsukh: Field data collection, Writing - Review, Altanbold Enkhbold: Writing - Review and editing

Complicit of interest

The authors declare that they have no conflict of interest. AI was used only for English grammar checking; all content, data, and interpretations are solely the authors' work.

REFERENCES

Abson, D.J., Dougill, A.J., Stringer, L.C. 2012. Using Principal Component Analysis for information-rich socio-ecological vulnerability mapping in Southern Africa. Applied Geography, vol. 35(1-2), p. 515-524. https://doi.org/10.1016/j.apgeog.2012.08.004

Altanbold, E., Ulambadrakh, K., Dash, D., Seong, Y.B., Batzorig, B., Gansukh, Y., Ser-Od, Ts. 2025. Delineating the boundary between the Mongolian Altay and Gobi-Altay Mountain Ranges: A Geomorphic and Geographical Approach. Geographical Issues, vol. 25(02), p. 115-137 (in Mongolian with English abstract) https://doi.org/10.22353/gi.2025.25.16

Amarjargal, S., Sainbuyan, B., HuGeJiLeTu, J., Narangerel, B., Sainbayar, D., Shiirev-Adiya, S. 2017. Land cover change in Mongolia (2001, 2015). Geography and Geoecological Issue in Mongolia, Special edition, vol. 2017(1), p. 186-194 (in Mongolian)

Baasan, T. 2008. The Sacred Highest Bogd Mountains of Mongolia (in Mongolian)

Badarch, N., Tsegmid, Sh., Tserensodnom, J. 1965. Tsegmid, Sh. (Ed.) The landscapes and natural zones of the eastern part of Mongolia. Ulaanbaatar, Mongolian Academy of Sciences Press, 117 p. (in Mongolian)

Batchuluun, Y. (Ed.) 2020. The Physical Geography of Mongolia. Ulaanbaatar, Munkhiin Useg, 480 p. (in Mongolian)

Bayasgalan, A., Jackson, J., Ritz, J-F., Carretier, S. 1999. Field examples of strike-slip fault terminations in Mongolia and their tectonic significance. Tectonics, vol. 18(3), p. 394-411. https://doi.org/10.1029/1999TC900007

Bento, V.A., Trigo, I.F., Gouveia, C.M., DaCamara, C.C. 2018. Contribution of land surface temperature (TCI) to vegetation health index: A comparative study using clear sky and all-weather climate data records. Remote Sensing, vol. 10(9), 1324. https://doi.org/10.3390/rs10091324

Bespalov, N.D. 1951. Soils of the People's Republic of Mongolia. Proceedings of the Mongolian Commission Moscow, Publishing House of the Academy of Sciences of the USSR, vol. 41, p. 13-15 (in Russian).

Bobrov, V.A., Baldan, S. Marinov, N.A. 1959. Gobi-Altai earthquake: December 4, 1957. Ulaanbaatar, 147 p. (in Mongolian).

Byamba, J., Baigalmaa, N., Khashbat, D. 2023. State-sacred Ikh Bogd Mountain: Geological History and Mineral Resources. In: Proceedings of the conference on Ikh Bogd Mountain: Sacred Sites and Offerings. Bayankhongor, Mongolia. (in Mongolian)

Caballero, I., Román, A., Tovar-Sánchez, A., Navarro, G. 2022. Water quality monitoring with Sentinel-2 and Landsat-8 satellites during the 2021 volcanic eruption in La Palma (Canary Islands). Science of The Total Environment, vol. 822, 153433. https://doi.org/10.1016/j.scitotenv.2022.153433

Cabello, J., Mairota, P., Alcaraz-Segura, D., Arenas-Castro, S., Escribano, P., Leitão, P.J. Martínez-López, J., Regos, A., Requena-Mullor, J.M. 2018. Satellite remote sensing of ecosystem functions: Opportunities and challenges for reporting obligations of the EU Habitat Directive. IGARSS 2018 - 2018 IEEE International Geoscience and Remote Sensing Symposium, p. 6604-6607. https://doi.org/10.1109/IGARSS.2018.8517296

Choi, J-H., Jin, K., Enkhbayar, D., Davvasambuu, B., Bayasgalan, A., Kim, Y-S. 2012. Rupture propagation inferred from damage patterns, slip distribution, and segmentation of the 1957 M_w

8.1 Gobi-Altay earthquake rupture along the Bogd fault, Mongolia. Journal of Geophysical Research: Solid Earth, vol. 117(B12), 401. https://doi.org/10.1029/2011JB008676

Dash, D. 2015. Landscape and Ecological Issues of Mongolia. Ulaanbaatar, Admon Print LLC, 264 p. (in Mongolian)

Davaa, G., Kadota, T., Purevdagva, K., Baasandorj, D. 2008. Preliminary results of study on flat-top glacier at Tsambagarav Mts. Mongolia. In: Proceedings of the International Conference on Uncertainties in Water Resource Management: Causes, Technologies and Consequences (WRM-Mon2008), p. 123-124. https://unesdoc.unesco.org/ark:/48223/pf0000163281

Dorjgotov, D. 2003. Soils of Mongolia. Ulaanbaatar, Admon Print, 287 p. (in Mongolian)

Duvjir, Ch. 1961. Ikh and Baga Bogd Mountains. Study of landscape and topography, Ulaanbaatar, Mongolia (in Mongolian)

Elizabeth, E. 2012. Mongolia's Regions: Lessons in Variation. In: A History of Land Use in Mongolia. Springer Nature, p. 23-42. https://doi.org/10.1057/9781137269669_2

Engle, N.L. 2011. Adaptive capacity and its assessment. Global Environmental Change, vol. 21(2), p. 647-656. https://doi.org/10.1016/j.gloenvcha.2011.01.019

Enkhbold, E., Khukhuudei, U., Seong, Y.B., Batbold, B., Tsedevdorj, S-O., Khandsuren, P., Ganbold, U., Gonchigjav, Y. 2026. Geomorphic characteristics of lake depressions in the Gobi-Altai Range, Mongolia: Impact of an earthquake-induced rockslide. Landslides, https://doi.org/10.1007/s10346-026-02805-x

Erickson, K.I., Leckie, R.L., Weinstein, A.M. 2014. Physical activity, fitness, and gray matter volume. Neurobiology of Aging, vol. 35(S2), p. S20-S28. https://doi.org/10.1016/j.neurobiolaging.2014.03.034

Ermida, S.L., Soares, P., Mantas, V., Göttsche, F-M., Trigo, I.F. 2020. Google Earth Engine open-source code for land surface temperature estimation from the Landsat series. Remote Sensing, vol. 12(9), 1471. https://doi.org/10.3390/rs12091471

Filei, A.A., Slesarenko, L.A., Boroditskaya, A.V., Mishigdorj, O. 2018. Analysis of desertification in Mongolia. Russian Meteorology and Hydrology, vol. 43(9), p. 599-606. https://doi.org/10.3103/S1068373918090066

Florensov, N.A., Solonenko, V.P. 1963. The Gobi-Altai earthquake. Moscow, Russian Academy of Sciences, 390 p. (in Russian)

Gbetibouo, G.A., Ringler, C. 2009. Mapping South African farming sector vulnerability to climate change and variability: A subnational assessment, International Food Policy Research Institute, IFPRI discussion paper 00885.

Hao, J., Lin, Q., Wu, T., Chen, J., Li, W., Wu, X., Hu, G., La, Y. 2023. Spatial-Temporal and Driving Factors of Land Use/Cover Change in Mongolia from 1990 to 2021. Remote Sensing, vol. 15(7), 1813. https://doi.org/10.3390/rs15071813

Hartmann, D.L., Klein Tank, A.M.G., Rusticucci, M., Alexander, L.V., Brönnimann, S., Charabi, Y., Dentener, F.J., Dlugokencky, E.J., Easterling, D.R., Kaplan, A., Soden, B.J., Thorne, P.W., Wild, M., Zhai, P.M. 2013. Observations: Atmosphere and Surface. In: Stocker, T.F., Qin, D., Plattner, G.-K., Tignor, M., Allen, S.K., Boschung, J., Nauels, A., Xia, Y., Bex, V., Midgley, P.M. (Eds.), Climate Change 2013: The Physical Science Basis. Working Group I Contribution to the Fifth Assessment Report of the Intergovernmental Panel on Climate Change. Cambridge University Press, p. 159-254. https://doi.org/10.1017/CBO9781107415324.008

Hilbig, W. 1995. The Vegetation of Mongolia. Amsterdam, SPB Academic Publishing, 258 p.

Hussain, S., Ahmad, A., Wajid, A., Khaliq, T., Hussain, N., Mubeen, M., Farid, H. U., Imran, M., Hammad, H. M., Awais, M., Ali, A., Aslam, M., Amin, A., Akram, R., Amanet, K., Nasim, W. 2020a. Irrigation scheduling for cotton cultivation. In: Ahmad, S., Hasanuzzaman, M. (Eds.), Cotton Production and Uses: Agronomy, Crop Protection, and Postharvest Technologies, Springer, Singapore, p. 59-80. https://doi.org/10.1007/978-981-15-1472-2_5

Hussain, S., Karuppannan, S. 2020b. Land use/land cover changes and their impact on land surface temperature using remote sensing technique in district Khanewal, Punjab, Pakistan. Geology, Ecology, and Landscapes, vol. 7(1), p. 46-58. https://doi.org/10.1080/24749508.2021.1923272

Jia, G., Shevliakova, E., Artaxo, P., De Noblet-Ducoudré, N., Houghton, R., House, J., Kitajima, K., Lennard, C., Popp, A., Sirin, A., Sukumar, R., Verchot, L. 2019. Land-climate interactions. In: Shukla, P.R., Skea, J., Calvo Buendia, E., Masson-Delmotte, V., Pörtner, H.-O., Roberts, D.C., Zhai, P., Slade, R., Connors, S., van Diemen, R., Ferrat, M., Haughey, S., Luz, S., Neogi, M., Pathak, J., Petzold, J., Portugal Pereira, P., Vyas, E., Huntley, E., Kissick, K., Belkacemi, M., Malley, J. (Eds.), Climate Change and Land. IPCC special report on Climate Change, Desertification, Land Degradation, Sustainable Land Management, Food Security, And Greenhouse Gas Fluxes In Terrestrial Ecosystems. 118 p. https://doi.org/10.1017/9781009157988.004

Johnson, D.L., Lewis, L.A. 2007. Land Degradation: Creation and Destruction. Second edition. Bloomsbury Academic, p. 303.

Kappas, M., Degener, J., Klinge, M., Vitkovskaya, I., Batyrbayeva, M.A. 2020. Conceptual Framework for Ecosystem Stewardship Based on Landscape Dynamics: Case Studies from Kazakhstan and Mongolia. In: Gutman, G., Chen, J., Henebry, G.M., Kappas, M. (Eds.), Landscape Dynamics of Drylands across Greater Central Asia: People, Societies and Ecosystems. Landscape Series, vol. 17, Springer, 143 p. https://doi:10.1007/978-3-030-30742-4_9

Kilpys, J., Rimkus, E., Byambasuren, O., Lkhamjav, J., Soyol-Erdene, T-O. 2025. Climate impact on the seasonal and interannual variation in NDVI and GPP in Mongolia. Atmosphere, vol. 16(11), 1307. https://doi.org/10.3390/atmos16111307

Kimuku, C.W., Ngigi, M.M. 2017. Study of Urban Heat Island Trends to Aid in Urban Planning in Nakuru County-Kenya. Journal of Geographic Information System, vol. 9(3), p. 309-325. https://doi.org/10.4236/jgis.2017.93019

Kozlov, P.K. 1925. Northern Mongolia-Noin-Ula monuments. In: Brief report of the expedition for the exploration of Northern Mongolia in connection with P.K. Kozlov's Mongolo-Tibetan Expedition. Leningrad, Academy of Sciences, USSR, p. 1-12 (in Russian).

Kurtz, R., Klinger, Y., Ferry, M., Ritz, J.F. 2018. Horizontal surface-slip distribution through several seismic cycles: The Eastern Bogd fault, Gobi-Altai, Mongolia. Tectonophysics, vol. 734-735, p. 67-182. 10.1016/j.tecto.2018.03.011

Lee, E.J., Piao, D., Song, C., Kim, J., Lim, C-H., Kim, E., Moon, J., Kafatos, M., Lamchin, M., Jeon, S.W., Lee, W-K. 2019. Assessing environmentally sensitive land to desertification using MEDALUS method in Mongolia. Forest Science and Technology, vol. 15(4), p. 210-220. https://doi.org/10.1080/21580103.2019.1667880

Mukherjee, F., Singh, D. 2020. Assessing Land Use-Land Cover Change and Its Impact on Land Surface Temperature Using LANDSAT Data: A Comparison of Two Urban Areas in India. Earth Systems and Environment, vol. 4(2), p. 385-407. https://doi.org/10.1007/s41748-020-00155-9

Murzaev, E.M. 1952. People's Republic of Mongolia: A Physical-Geographical Description. Moscow, State Publishing House of Geographical Literature, p. 13-18 (in Russian).

Narangarav, D., Lin, C. 2011. Investigation of vegetation dynamics of Mongolia using time series of NDVI in response to temperature and precipitation. Mongolian Journal of Biological Sciences, vol. 9(1-2), p. 9-17. https://doi.org/10.22353/mjbs.2011.09.02

O'Brien, K., Leichenko, R., Kelkar, U., Venema, H., Aandahl, G., Tompkins, H., Javed, A., Bhadwal, S., Barg, S., Nygaard, L., West, J. 2004. Mapping vulnerability to multiple stressors: climate change and globalization in India. Global Environmental Change, vol. 14(4), p. 303-313 https://doi.org/10.1016/j.gloenvcha.2004.01.001

Otgonbayar, M., Atzberger, C., Mattiuzzi, M., Erdenedalai, A. 2019. Estimation of Climatologies of Average Monthly Air Temperature over Mongolia Using MODIS Land Surface Temperature (LST) Time Series and Machine Learning Techniques. Remote Sensing, vol. 11(21), 2588. https://doi.org/10.3390/rs11212588

Perminova, T., Sirina, N., Laratte, B., Baranovskaya, N., Rikhvanov, L. 2016. Methods for land use impact assessment: A review. Environmental Impact Assessment Review, vol. 60, p. 64-74. https://doi.org/10.1016/j.eiar.2016.02.002
Rachkovsky, I.P., Lebedeva, Z.A. 1932. Summary of the work of the geological unit of the expedition of the USSR Academy of Sciences and the Research Committee of the People's Republic of Mongolia in 1931. In: Proceedings of the Mongolian Commission, Leningrad, USSR Academy of Sciences Publishing House, vol. 6, p. 1-28 (in Russian).
Rani, M., Kumar, P., Pandey, P.C., Srivastava, P.K., Chaudhary, B.S., Tomar, V., Mandal, V.P. 2018. Multi-temporal NDVI and surface temperature analysis for urban heat Islandinbuilt surrounding of sub-humid region: A case study of two geographical regions. Remote Sensing Applications: Society and Environment, vol. 10, p. 163-172. https://doi.org/10.1016/j.rsase.2018.03.007
Rizza, M., Ritz, J-F., Braucher, R., Vassallo, R., Prentice, C., Mahan, S., McGill, S., Chauvet, A., Marco, S., Todbileg, M., Demberel, S., Bourlès, D. 2011. Slip rate and slip magnitudes of past earthquakes along the Bogd left-lateral strike-slip fault (Mongolia). Geophysical Journal International, vol. 186(3), p. 897-927. https://doi.org/10.1111/j.1365-246X.2011.05075.x
Sandholt, I., Rasmussen, K., Andersen, J. 2002. A simple interpretation of the surface temperature/vegetation index space for assessment of surface moisture status. Remote Sensing of Environment, vol. 79(2-3), p. 213-224. https://doi.org/10.1016/S0034-4257(01)00274-7
Simukov, A.D. 1936. Results of 15 Years of Work of the Geographical Section of the Research Committee of the People's Republic of Mongolia. Contemporary Mongolia, vol. 4-5(17-18), p. 67-86 (in Russian).
Smirnov, V.A. 1932. Report on the work of the hydrochemical unit of the Mongolian expedition, 1926. In: Proceedings of the Mongolian Commission, Leningrad, Publishing House of the Academy of Sciences of the USSR, vol. 1, p. 1-23, (in Russian).
Stelzenmüller, V., Coll, M., Mazaris, A.D., Giakoumi, S., Katsanevakis, S., Portman, M.E., Degen, R., Mackelworth, P., Gimpel, A., Albano, P.G., Almpanidou, V., Claudet, J., Essl, F., Evagelopoulos, T., Heymans, J.J., Genov, T., Kark, S., Micheli, F., Pennino, M.G., Rilov, G., Rumes, B., Steenbeek, J., Ojaveer, H. 2018. A risk-based approach to cumulative effect assessments for marine management. Science of The Total Environment, vol. 612, p. 1132-1140. https://doi.org/10.1016/j.scitotenv.2017.08.289
Terbish, Kh. Jamsran, Ts. (Eds.). 2006. Ikh Bogd. Geology, landscape, and biodiversity. Ulaanbaatar, Gan Print, 140 p. (in Mongolian)
Tsedevdorj, S-O. 2021. Glaciers of Mongolia. In: Yembuu, B. (Ed.), The Physical Geography of Mongolia. Geography of the Physical Environment, Springer, p. 101-117 https://doi.org/10.1007/978-3-030-61434-8_6
Tsedevdorj, S-O., Doljin, D., Ganbold, U. 2024. Geographical characteristics of Ikh Bogd Mountain and the impact of climate change. Geoforum Journal, vol. 14(1), p. 23-28. (in Mongolian with English abstract) https://geoforum.mn/mn/104/0/47
Tsedevdorj, S-O., Khurelbaatar, T., Ganbold, U., Yadamsuren, G., Avkhinsukh, A., Erkhembayar, B., Zhang, W., Enkhbold, A. 2025. Climate change impact of land cover changes in the Kharhiraa-Turgen mountain region. Mongolian Geoscientist, vol. 30(61), p. 1-13. https://doi.org/10.5564/mgs.v30i61.3866
Tsegmid, S. 1969. Physical Geography of Mongolia. Ulaanbaatar. Institute of Geography and Permafrost Studies, Mongolian Academy of Sciences, Ulaanbaatar, State Press, 405 p. (in Mongolian).
Ulziikhutag, N. 1989. Overview of the flora of Mongolia. Ulaanbaatar, State Publishing House, 208 p. (in Mongolian).
World Bank. 2009. Climate Risk Country Profile: Mongolia. Washington, DC, World Bank.
Yunatov, A.A. 1948. Vegetation of the Mongolian People's Republic. Publishing House of the Academy of Sciences of the USSR, Moscow–Leningrad, 223 p. (in Russian)